Available online at www.sciencedirect.com
ScienceDirect
Journal of the European Ceramic Society 27 (2007) 3183–3190
www.elsevier.com/locate/jeurceramsoc

Kinematics of a single abrasive particle during the industrial polishing process of porcelain stoneware tiles

Fábio J.P. Sousa [a,*], Jan C. Aurich [b], Walter L. Weingaertner [c], Orestes E. Alarcon [c]

[a] *Postgraduate Program in Material Science Engineering (PGMat/EMC/LabMat), Federal University of Santa Catarina (UFSC), Department of Mechanical Engineering, Campus Universitário Trindade, LabMat, EMC-B, Postcode 88040-900, CP 476, Florianópolis, SC, Brazil*
[b] *Institute for Manufacturing Engineering and Production Management, University of Kaiserslautern, PO Box 3049, D-67653 Kaiserslautern, Germany*
[c] *Department of Mechanical Engineering, EMC, Federal University of Santa Catarina (UFSC), Postcode 88040-900, CP 476, Florianópolis, SC, Brazil*

Received 7 October 2006; received in revised form 9 December 2006; accepted 16 December 2006
Available online 28 February 2007

Abstract

In order to achieve glossiness the porcelain stoneware tiles must undergo an industrial polishing process, which can be optimized by either the scratching phenomena or the polishing kinematics. This paper is focused on the latter. Thus, the most important kinematic equations involved in polishing process were described. The lateral oscillation used in modern polishing machines, as well as the other available motions were taken into account. The trajectory of abrasives, the scratching speed and the curvature radius could be obtained for each instant. The importance of adopting good kinematics parameters for the accomplishment of the polishing process was highlighted, and the equations furnished hereby serve as useful tools for further attempts in optimizing the polishing process.

Keywords: Finishing; Surfaces; Wear resistance; Porcelain; Polishing process; Tiles

1. Introduction

Polishing is a common process in stoneware floor tile production, due to the exceptional aesthetic resulting effect. Nevertheless, the industrial polishing process usually bases on trial and error or, despite of the systemic character inherent of abrasive process,[1] on experience obtained from others materials such as natural stones, i.e., marble or granite.[2–4]

The necessity of researches on polishing process, with either scientific or technologic point of view, is highlighted considering the high operation costs involved. In stoneware tile manufacturing the polishing step stands for 30–40% of final cost.[5,7]

Nevertheless, many successful works on the attempt of improving the polishing process,[2,3,5,6] or even only kinematic optimization of lapping machines,[8,9] are available in literature for glassy materials. The present work intends to analyze the kinematics involved in the porcelain stoneware tile polishing, in order to furnish further data on this subject, considering the operational parameters usually available by industries.

Polishing is a common term used in several ways, but always with the connotation of increasing the gloss of a given surface. However, from a technical point of view, polishing is a machining process with almost no material removal, promoted by free abrasive particles, whose shape is not individually defined. Moreover, the material to support these particles must be quite soft, like cotton or leather, since the goal is to give glossiness to the surface, instead of shaping it. The softness of the support causes the abrasives to scratch the surface with a minimal penetration, hence giving the desired glossy appearance. In the case of porcelain stoneware tiles, it must be mentioned that the highest gloss that can be obtained by an industrial polishing line is limited by the superficial microstructure.[3,10,11]

As described elsewhere,[2,3,5,6] in industries commonly more than twenty polishing machines can be disposed in sequence to comprise an industrial polishing line. In each polishing machine there is a disk compounded by a horizontal spinning plate in which six abrasive blocks are coupled keeping a radial symmetry. These abrasive blocks, in turn, consists of silicon carbide particles embedded in a magnesium oxychloride cement matrix.[5–7]

Previous studies[5] detected that during polishing some regions over the tile surface are favored on material removal and hence

* Corresponding author. Tel.: +49 631 205 2872; fax: +49 631 205 3238.
E-mail address: sousa@cck.uni-kl.de (F.J.P. Sousa).

0955-2219/$ – see front matter © 2007 Elsevier Ltd. All rights reserved.
doi:10.1016/j.jeurceramsoc.2006.12.007

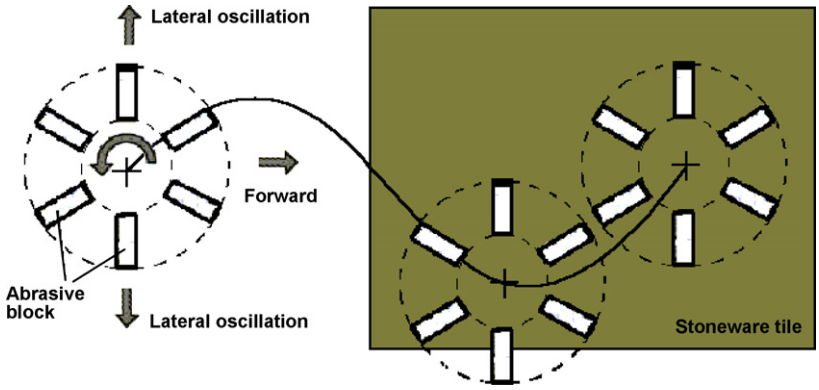

Fig. 1. Plan view of the relative motion of an abrasive head for modern polishing machines.

on gloss gaining. For simple polishing machines, this fact is promptly ascribed to the lack of abrasives in the center of the abrasive heads, i.e., between two radially opposed abrasive blocks. However, apart from the abrasive lacking, such fact can be also interpreted as being consequence of the available kinematics.

In simple polishing machines, the abrasive blocks accomplish only the spinning and the forward movement, whereas in modern polishing machines, there is also the motion offered by the lateral oscillation of the polishing head. The final relative movement is presented in Fig. 1.

Thus, for modern polishing machines the problems caused by lack of abrasives in the middle of polishing heads is reduced, since it remains no longer at the same position over the tile surface. The favoring on material removal during polishing by modern polishing machines was not found in the literature surveyed. However, considering the available motion described above, it can be showed that a zigzag overlapping pattern comes out for a single abrasive particle, as illustrated in Fig. 2.

Fig. 2 shows a continuous scratch caused by the most inner abrasive for a given abrasive block, during some extend of the polishing process. However, this pattern should not be taken as a final pattern, since all the others abrasives must be also considered. This graphic was analytically determined using the premises detailed in the next section.

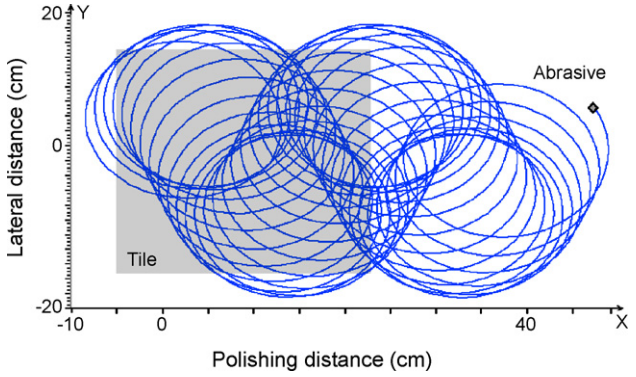

Fig. 2. Trajectory of a single abrasive along the polishing line.

2. Kinematics equations

Kinematics mainly deals with the motion accomplished by a given body, without considering the forces involved. The available motion of the polishing machine, as showed in Fig. 1, governs the abrasive trajectory over the tile surface. This trajectory, and consequently the position of the abrasive particles for each instant (t [s]), can be analytically determined, depending on the following operational parameters: rotational speed of the abrasive disk (w [rpm]), forward speed of the polishing line (V [cm s^{-1}]), frequency of the lateral oscillation (f [s^{-1}]), lateral oscillation amplitude (A [cm]), and the distance from the chosen particle to the center of the abrasive head (r [cm]).

In addition to the motion sources mentioned so far, each abrasive block accomplishes a swinging motion around its own longitudinal axis in order to keep a homogeneous consumption of abrasive. However, although this swinging promotes the movement of all the abrasive particles, it tends to cause no further displacement of the effective contact zone, as illustrated in Fig. 3.

First, an axis reference system was adopted, in which the unitary vector $\hat{\mathbf{i}}$ is parallel to the forward direction of the tile. Another unitary vector $\hat{j}$ stands for the direction of the lateral oscillation, i.e., perpendicular and belonging to the same plane that vector $\hat{\mathbf{i}}$.

The displacement vector ($\vec{D}$) of the abrasive at instant t_0 results from the contribution of each source of motion: forwarding of the tile ($\vec{D}E$), rotation ($\vec{D}R$) and lateral oscillation of the abrasive disk ($\vec{D}OL$). The reference axis, as well as each component of the displacement vector, for a given instant t_0, can be seen in Fig. 4.

In vector form $\vec{D}$ can be expressed as

$$\vec{D} = f(w, r, A, f, V, t) = \vec{D}E + \vec{D}R + \vec{D}OL \quad (1)$$

where

$$\vec{D}E = f(V, t) = \{V \cdot t\}\hat{\mathbf{i}} + \{0\}\hat{\mathbf{j}} \quad (2)$$

$$\vec{D}R = f(W, r, t) = \{r \cdot \cos(w \cdot t)\}\hat{\mathbf{i}} + \{r \cdot \sin(w \cdot t)\}\hat{\mathbf{j}} \quad (3)$$

$$\vec{D}OL = f(A, f, t) = \{0\}\hat{\mathbf{i}} + \left\{\frac{A}{2} \cdot \sin(2 \cdot \pi \cdot f \cdot t)\right\}\hat{\mathbf{j}} \quad (4)$$

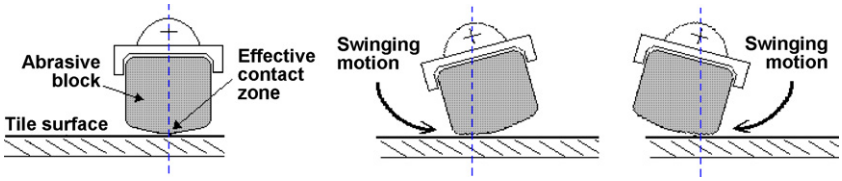

Fig. 3. Null effect of the swinging motion on the displacement of the effective contact zone.

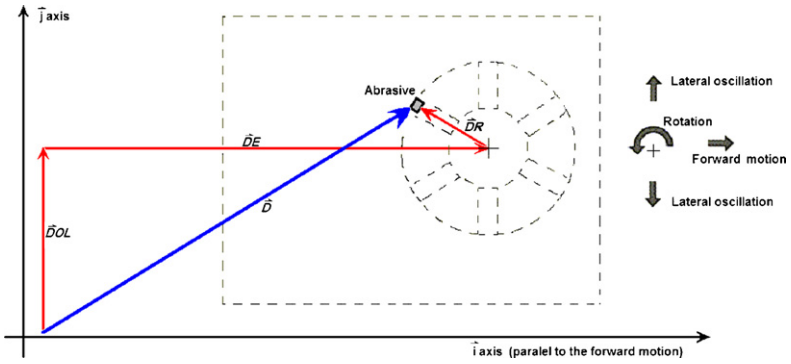

Fig. 4. Resulting displacement vector and its components for a single abrasive.

which results in the following:

$$\vec{D} = \{V \cdot t + r \cdot \cos(w \cdot t)\}\hat{\mathbf{i}} + \left\{r \cdot \sin(w \cdot t) + \frac{A}{2} \cdot \sin(2 \cdot \pi \cdot f \cdot t)\right\}\hat{\mathbf{j}} \quad (5)$$

Contribution of the vectors $\vec{D}E$, $\vec{D}R$ and $\vec{D}OL$ to the displacement, plotted against time are presented in Fig. 5a and b, concerning to directions $\hat{\mathbf{i}}$ and $\hat{j}$, respectively. The required parameters were adopted as followed: $W = 450$ rpm, $V = 7.5\,\mathrm{cm\,s^{-1}}$, $f = 0.4\,\mathrm{s^{-1}}$, $A = 15$ cm and $r = 11$ cm.

Rotation component $\vec{D}R$ influences the position of the abrasive at both directions, whereas forward and lateral oscillation motions acts only at one direction, $\hat{\mathbf{i}}$ or $\hat{j}$, respectively.

Eq. (5) assemblies all those contributions and its behavior can be seen in Fig. 2, which uses the same polishing condition detailed above. Hence this equation can be promptly used to predict the position of a given abrasive particle for any instant, as well as the whole path, in which the abrasive goes through along the polishing process.

Although this path becomes slightly different according to the distance taken between abrasive and center of polishing head, i.e., the radius r, it gives a reasonable idea of the favored polishing pattern undergone by a surface.

The velocity vector $\vec{\vartheta}$, in which the abrasive scratches the tile surface, can be achieved by taking derivative of Eq. (5) with respect to time. This derivative yields Eq. (6), whose modulus stands for the scratching speed, υ, given by Eq. (7). Contribution due to the swinging motion could be added directly into the scratching speed, since it has always the same direction of the instantaneous scratching velocity:

$$\vec{\vartheta} = \frac{\mathrm{d}\vec{D}}{\mathrm{d}t} = \{V - r \cdot w \cdot \sin(w \cdot t)\}\hat{\mathbf{i}} + \{r \cdot w \cdot \cos(w \cdot t) + A \cdot f \cdot \pi \cdot \cos(2 \cdot \pi \cdot f \cdot t)\}\hat{\mathbf{j}} \quad (6)$$

$$\upsilon = |\vec{\vartheta}| = |\{V - r \cdot w \cdot \sin(w \cdot t)\}\hat{\mathbf{i}} + \{r \cdot w \cdot \cos(w \cdot t) + A \cdot f \cdot \pi \cdot \cos(2 \cdot \pi \cdot f \cdot t)\}\hat{\mathbf{j}}| \quad (7)$$

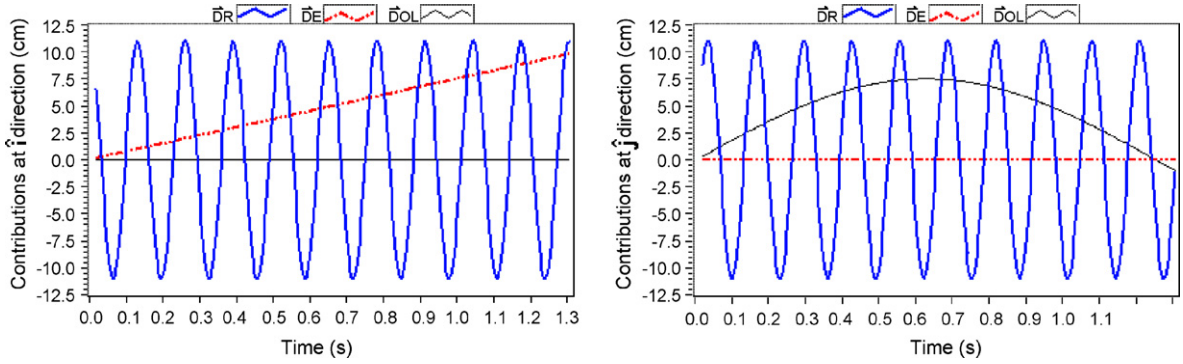

Fig. 5. Values of vectors $\vec{D}E$, $\vec{D}R$ and $\vec{D}OL$ along time, regarding to directions: (a) $\hat{\mathbf{i}}$ and (b) $\hat{j}$.

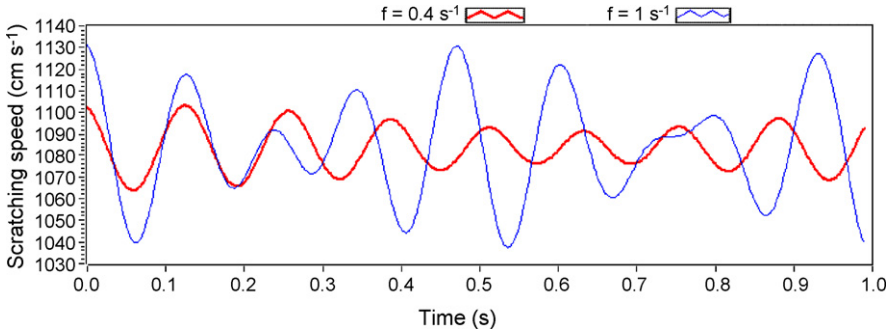

Fig. 6. Peripheral scratching speed along polishing for two different lateral oscillation frequencies.

The variation of the scratching speed for an outmost abrasive particle ($r = 23$ cm) can be seen in Fig. 6. The others parameters were the same as adopted in Fig. 5. Additionally, an extra value of lateral oscillation frequency was included, so that its contribution on the scratching speed could be noted.

The most important source of speed during the scratching is by far the rotational movement. The lateral oscillation frequency accounts for much less in the speed increasing. The range of values achieved was slightly higher than those previously indicated in literature,[6] which was about 800 cm s^{-1}.

From the ratio between both multiplicative terms of $\hat{\mathbf{i}}$ and $\hat{j}$ unitary vectors, Eq. (7) furnishes the scratching orientation for each instant, as illustrated in Fig. 6, and described in Eq. (8):

$$\tan(\varphi) = \frac{\Delta y\hat{\mathbf{j}}}{\Delta x\hat{\mathbf{i}}} = \frac{\{r \cdot w \cdot \cos(w \cdot t) + A \cdot f \cdot \pi \cdot \cos(2 \cdot \pi \cdot f \cdot t)\}}{\{V - r \cdot w \cdot \sin(w \cdot t)\}} \quad (8)$$

Fig. 7 presents the behavior of the scratching angle. The reference line was always taken as the forward polishing direction. Apart from the values used in Fig. 5, an overstated value of lateral oscillation frequency was exceptionally included in Fig. 7 in order to highlight the small effect of this variable on the scratching orientation. The corresponding trajectory of both cases: (a) $f = 0.4$ s^{-1} and (b) $f = 3$ s^{-1} were also presented and one might note the great influence of variable f over the path of the abrasive.

The second order time derivative of Eq. (6) with time stands for the acceleration of particle, given by Eq. (9):

$$\vec{a} = \frac{d\vec{\vartheta}}{dt} = -\{r \cdot w^2 \cdot \cos(w \cdot t)\}\hat{\mathbf{i}} - \{r \cdot w^2 \cdot \sin(w \cdot t) + 2 \cdot A \cdot f^2 \cdot \pi^2 \cdot \sin(2 \cdot \pi \cdot f \cdot t)\}\hat{\mathbf{j}} \quad (9)$$

Since the abrasive describes a nonrectilinear movement, the direction of the vector $\vec{a}$ is not the same as $\vec{\vartheta}$.

3. Curvature radius of the scratches

Another important parameter that can be predicted according to the adopted kinematics is the radius of curvature ρ, in which the abrasive scratches the surface of the porcelain stoneware tile during the polishing process. In view of this it is suggested[12] to write Eq. (9) in a most appropriate way, so that ρ can be directly attained.

As shown in Fig. 8, the same vector $\vec{a}$ can be represented using the reference axis $\vec{\eta}$ and $\vec{\tau}$. Each one of these axis has its correspondent unitary vector $\hat{\eta}$ and $\hat{\tau}$, and differently from the former axis, the directions of these vectors vary in time. However, on the other hand they stay always parallel and perpendicular to $\vec{\vartheta}$, respectively.

Since vector $\vec{\tau}$ has always the same direction of $\vec{\vartheta}$, it can be written:

$$\vec{\vartheta} = \upsilon \cdot \hat{\tau} \quad (10)$$

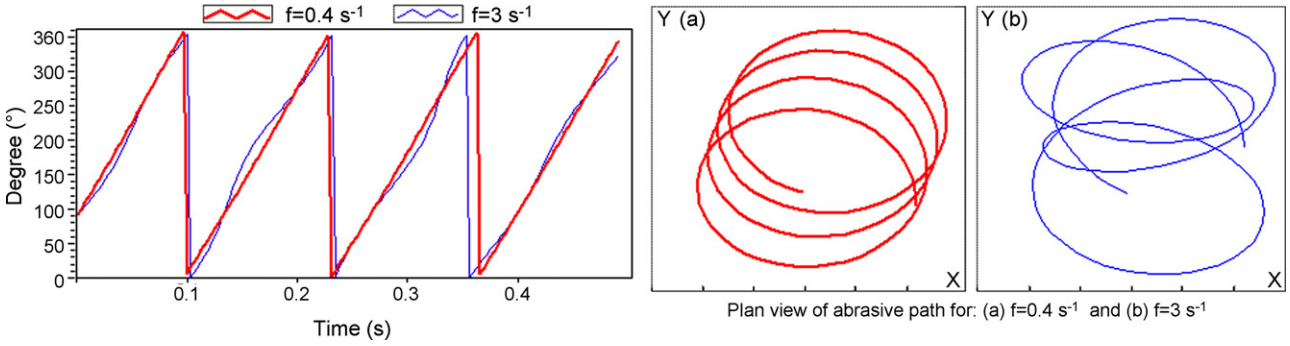

Fig. 7. Scratching angle (in degree) and abrasive path for different values of lateral oscillation frequencies.

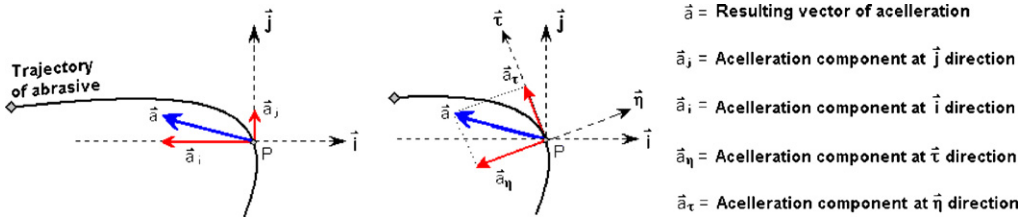

Fig. 8. Changing of reference axis.

According to the rules of differentiation, the acceleration vector can be also given by Eq. (11):

$$\vec{a} = \frac{d\vec{\vartheta}}{dt} = \frac{d\upsilon}{dt} \cdot \hat{\tau} + \upsilon \cdot \frac{d\hat{\tau}}{dt} \tag{11}$$

The determination ρ by means of Eq. (11) can be explained with the aid of Fig. 9. As the increment Δt decreases, it can be seen that the variation of vector $\hat{\tau}$ ($\Delta\vec{\tau} = \vec{\tau}_2 - \vec{\tau}_1$) and the variation of angle $\Delta\theta$ decrease simultaneously. Besides, $\Delta\vec{\tau}$ also becomes perpendicular to $\hat{\tau}$. It follows that in the limit, while Δt tends to zero, the ratio $d\hat{\tau}/d\theta$ yields the unit vector $\hat{\eta}$. In addition, the radius of curvature ρ can be written as the ratio between the arc of length dL and angle $d\theta$.

Thus, the last term in Eq. (11) is further modified, so that it could be written purely in terms of $\hat{\eta}$ and $\hat{\tau}$ goes on by using the chain rule, as follows:

$$\frac{d\hat{\tau}}{dt} = \frac{d\hat{\tau}}{d\theta} \cdot \frac{d\theta}{dt} \tag{12}$$

The ratio $d\theta/dt$ can be still changed by applying the chain rule second time:

$$\frac{d\theta}{dt} = \frac{d\theta}{dL} \cdot \frac{dL}{dt} \tag{13}$$

And replacing $d\theta/dt$ from Eq. (12) in Eq. (13):

$$\frac{d\hat{\tau}}{dt} = \frac{d\hat{\tau}}{d\theta} \cdot \frac{d\theta}{dL} \cdot \frac{dL}{dt} \tag{14}$$

Taking into account that $\rho = dL/d\theta$, $\hat{\eta} = d\hat{\tau}/d\theta$ and $\upsilon = dL/dt$, it can be written that:

$$\vec{a} = \frac{d\upsilon}{dt} \cdot \hat{\tau} + \frac{\upsilon^2}{\rho} \cdot \hat{n} \tag{15}$$

Finally, after replacing the required functions regarding the polishing process, ρ can be achieved as follows:

$$\rho = \left\{ \frac{\alpha^3}{\beta \cdot \alpha - (\varepsilon - \gamma)^2} \right\}^{1/2} \tag{16}$$

where:

$$\alpha = V^2 - 2 \cdot V \cdot r \cdot w \cdot \sin(w \cdot t) + r^2 \cdot w^2 + 2 \cdot r \cdot w \cdot A \cdot f \cdot \pi \cdot \cos(2 \cdot \pi \cdot f \cdot t) + [A \cdot f \cdot \pi \cdot \cos(2 \cdot \pi \cdot f \cdot t)]^2 \tag{17}$$

$$\beta = r^2 \cdot w^4 + 2 \cdot A \cdot r \cdot \pi^2 \cdot f^2 \cdot w^2 \cdot \sin(w \cdot t) \cdot \sin(2 \cdot \pi \cdot f \cdot t) + [2 \cdot A \cdot \pi^2 \cdot f^2 \cdot \sin(2 \cdot \pi \cdot f \cdot t)]^2 \tag{18}$$

$$\varepsilon = -V \cdot r \cdot w^2 \cdot \cos(w \cdot t) - r \cdot w^2 \cdot A \cdot f \cdot \pi \cdot \sin(w \cdot t) \cdot \cos(2 \cdot \pi \cdot t) \tag{19}$$

$$\gamma = 2 \cdot r \cdot w \cdot A \cdot f^2 \cdot \pi^2 \sin(2 \cdot \pi \cdot f \cdot t) \cdot \cos(w \cdot t) + 2 \cdot A^2 \cdot f^3 \cdot \pi^3 \cdot \sin(2 \cdot \pi \cdot f \cdot t) \cdot \cos(2 \cdot \pi \cdot f \cdot t) \tag{20}$$

The behavior of Eq. (16) can be seen in Fig. 10 by keeping the same polishing conditions used previously, but including an extra value of lateral oscillation frequency, $f = 1\ s^{-1}$. In both cases, certain periodicity was found and the instantaneous radius of curvature stayed centered in the vicinity of 11 cm, which is in fact the value adopted for r. A range of variation between 10 and 12 cm was found for a frequency $f = 0.4\ s^{-1}$, whereas frequency $f = 1\ s^{-1}$ has caused a variation of radius values from 9 up to 13.5 cm.

4. Macro kinematics of the polishing lines

Considering the fact that in the industrial polishing machines all the polishing heads accomplish the same movement in a syn-

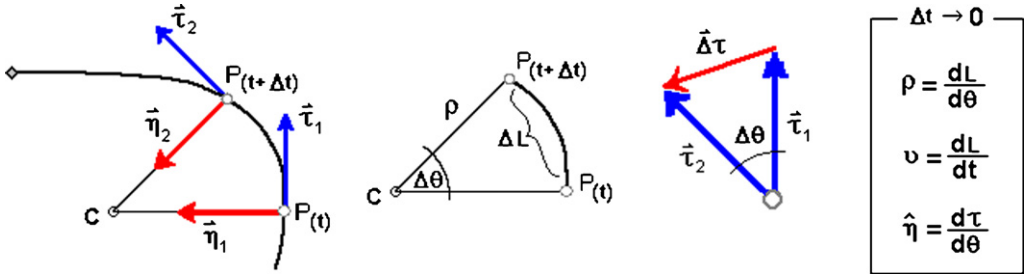

Fig. 9. Determination of ρ from vector $\vec{\eta}$.

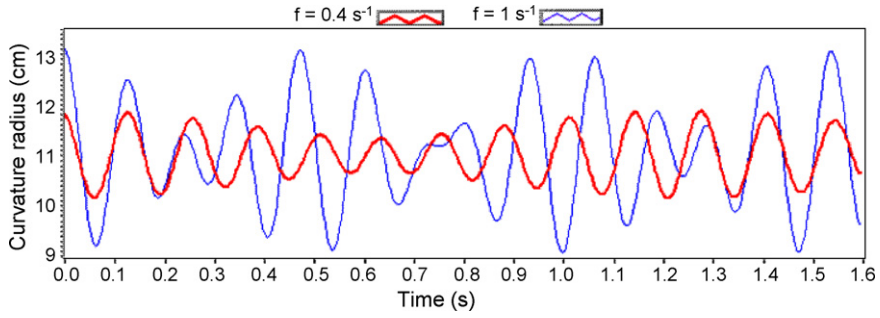

Fig. 10. Radii of curvature described by an abrasive particle during the polishing process.

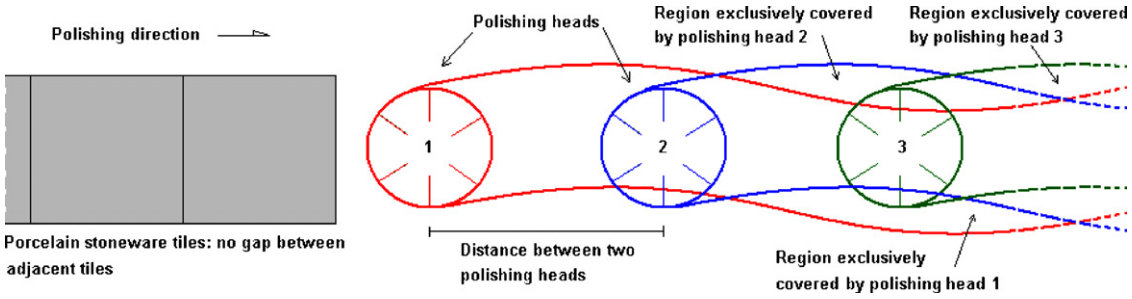

Fig. 11. Overlapping of areas covered by three adjacent polishing heads.

chronized way and the distances between two adjacent polishing heads are known and fixed, the set of polishing heads can be interpreted as coherent waves, in the sense that only phase difference between them can exist. The overlapping of the regions covered by three polishing heads is sketched in Fig. 11.

As indicated by Fig. 11, due to the lateral oscillation motion there can be regions somewhere along the tile surface being touched exclusively by one of the whole polishing head set, or even by no one from the whole polishing set. In addition, there must be no gap between the porcelain tiles while they are being driven toward the polishing in order to avoid an abrupt re-entrance of the abrasive block over the proper surface of the tile, which very often leads to coarse scratches.

This set of three polishing heads can represent polishing heads with the same abrasive size, which occurs often in industries. Thus, the importance of the total covered area rises due to the difficulty found by the next polishing heads in reducing the damages left by the previous stages, since coarser abrasives were adopted.

Similar to the path of each abrasive particle, the amount of overlapping area can be predicted by means of kinematic features, considering in addition the distance H between adjacent polishing heads. The others main features adopted in this macro kinematics modelling are illustrated in Fig. 12.

Since the time required for one complete cycle of the lateral oscillation is directly given by $T = 1/f$, the wave length λ can be achieved by multiplying this time with the forward speed V, so that:

$$\lambda = \frac{V}{f} \tag{21}$$

In accordance with Fig. 12, the following general function can be written:

$$Y_i = \frac{A}{2} \cdot \sin\left[\frac{X + (i-1)}{\lambda} \cdot 2\pi\right] \tag{22}$$

where $i \in N$ represents the number of the polishing head, and H is the distance between two adjacent polishing heads, often fixed

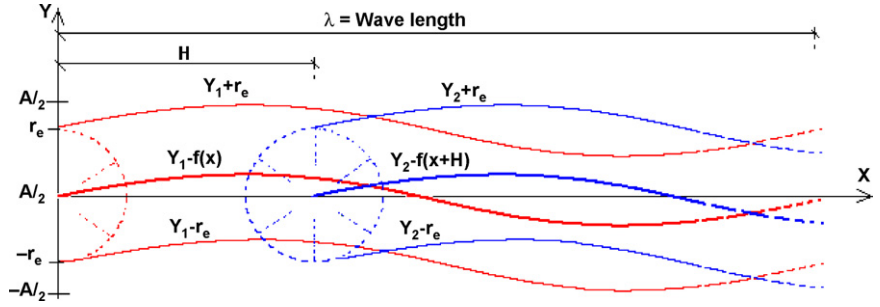

Fig. 12. Features adopted to evaluate the covering area for each polishing head.

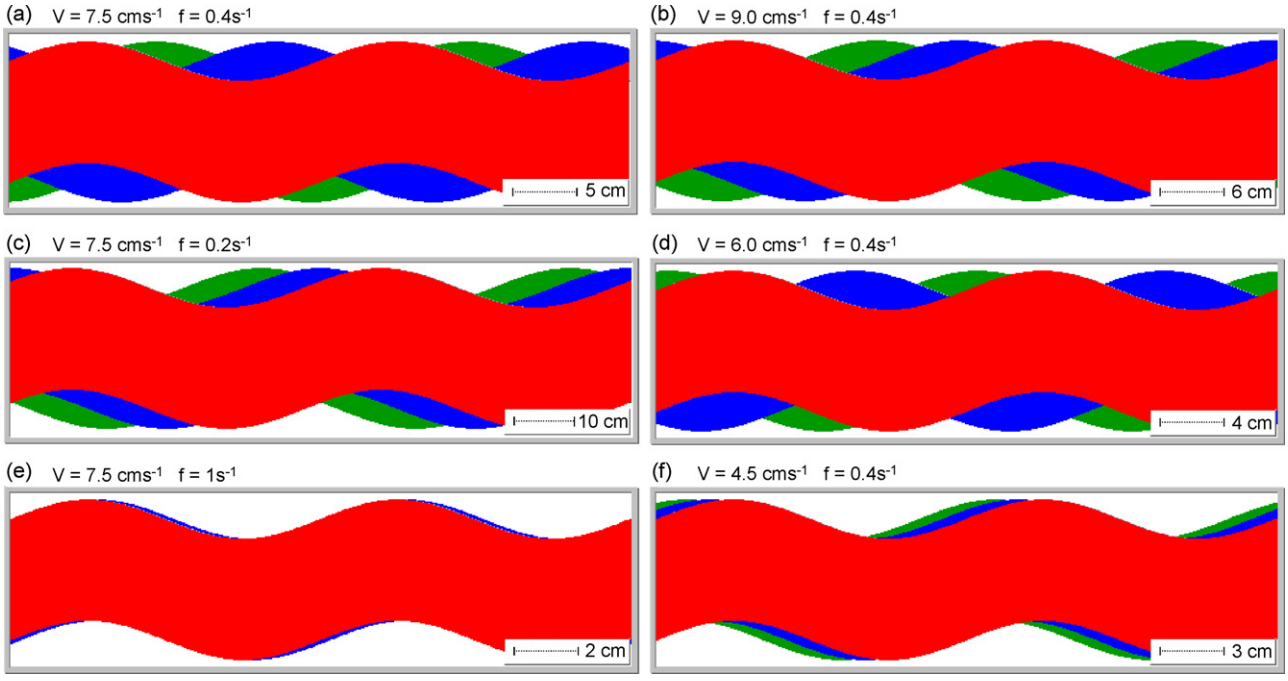

Fig. 13. (a–f) Overlapping pattern from three polishing machines adopting various kinematics conditions.

at about 55 cm. Considering the sensibility of sine functions, it follows from Eq. (17) that the role of either V or f on the overlapping amount of adjacent polishing heads are not that obvious to comprehend, especially by using trial and error approach. The results for six different kinematic conditions are given in Fig. 13.

As can be seen in Fig. 13(a), the condition typically used in both industries or in literature[5,6] seems to cover the whole surface of the porcelain stoneware tiles very well. However, noteworthy is the fact that, although it is commonly expected that increasing the lateral oscillation frequency improves the overlapping pattern, it is not necessarily so, and it can even lead to poorer covering pattern, as observed in Fig. 13(e).

In the same way, a reduction of the forward speed can also lead to regions which are poorly covered by the whole set of polishing head. A comparison between graphic Fig. 13(b) and (f) reveals that a better coverage would be achieved by using a forward speed two times faster as used in Fig. 13(f), so that a double productivity would be rather possible.

5. Conclusions

The kinematic features involved in the industrial polishing process were analyzed and the corresponding equations accounting for modern polishing machines were established. The possibility of assessing the instantaneous position of a given abrasive particle, as well as the scratching speed and its curvature radius becomes a useful guideline for further simulations of the polishing process.

The scratching behavior achieved for one single abrasive particle indicated a zigzag pattern in the material removal over the porcelain tile surface. However, this pattern should not be readily taken as a final pattern, since all the other abrasives must be also considered.

Regarding the macro kinematics involved in the industrial polishing process, it was found that the ratio between the forward speed and the lateral oscillation frequency plays an important role to indicates the number of polishing heads that might have the same abrasive size along the production line since it defines the amount of overlapping between areas covered by adjacent polishing heads.

Nevertheless, great sensitivity was found in the relation between such overlapping patterns and the kinematics adopted. Hence little success is expected by using trial an error approach to optimize the polishing process.

In addition, it was found that an increase in the frequency of lateral oscillation does not necessarily lead to a better overlapping pattern. Analogously, a decrease in forward speed does not always imply in a better overlapping either.

Finally, experimental studies are know needed to understand the effects of the kinematics on the interaction of abrasive and tile surface.

Acknowledgments

This work was carried out with the support of The National Council for Scientific and Technological Development (CNPq), an entity from the Brazilian Government.

Authors would also like to formally thank for the suggestion given by M.Sc. Halil Bil, co-worker at the Institute for Manufacturing Engineering and Production Management, FBK, University of Kaiserslautern, Germany.

References

1. Karl-Hein and Gahr, Z., *Microstructure and Wear of Materials, Tribology Series 10*. Elsevier Science Publishers B.V., Amsterdam, The Netherlands, 1987.

2. Ibáñes, M. J., Sánchez, E., García-Ten, J., Orts, M. J., Cantavella, V., Sánchez, J., Soler, C., Portolés, J. and Sales, J., *Use of a Pin-on-Disk Tribometer for Studying Porcelain Tile Polishing*. QUALICER, Castelón, Spain, 2002, pp. 32–49.
3. Tucci, A. and Espósito, L., *Polishing of Porcelain Stoneware Tile: Surface Aspects*. QUALICER, Castelón, Spain, 2000, pp. 127–136.
4. Nogueira, R. E. F. Q. and Mello, J. D. B., Avaliação do comportamento em abrasão de granitos naturais utilizando esclerometria pendular [Evaluation of the wear behavior of natural granites by pendular sclerometry]. In *IV Seminário Brasileiro de Materiais Resistentes ao Desgaste* [Brazilian Seminar of Wear Resistance Materials]. São Paulo, SP, 1998, pp. 249–261.
5. Hutchings, I. M., Adachi, K., Xu, Y., Sánches, E. and Ibáñez, M. J., *Laboratory Simulation of the Industrial Ceramic Tile Polishing Process*, QUALICER, Castelón, Spain, 2004, pp. 19–30.
6. Hutchings, I. M., Adachi, K., Xu, Y., Sánchez, E., Ibáñez, M. J. and Quereda, M. F., Analysis and laboratory simulation of an industrial polishing process for porcelain ceramic tiles. *J. Eur. Ceram. Soc.*, 2005, 3151–3156.
7. Espósito, L., Tucci, A. and Naldi, D., The reliability of polished porcelain stoneware tiles. *J. Eur. Ceram. Soc.*, 2005, 785–793.
8. Universitat Bremen, Rwth Aachen und Oklahoma State: Transregionaler Sonderforschungsbereich, Prozessketten zur replication komplexer optikkomponenten SFB/TR4. Teilprojekt F4: Maschinenseitige Aspekte des Scheifens und Polierens von Prazisionsformen aus Stahl und Keramik, Veroffentlichungen. Annals of the German Scientific Society of Production Technology WGP, 2004.
9. Aurich, J. C., Warnecke, G. and Braun, O., Kinematische Simulation zur Prozessoptimierung und Werkzeugentwicklung beim Schleifen. In: Jahrbuch "Schleifen, Honen, Läppen und Polieren", 61. H. -W. Hoffmeister and H. -K. Tönshoff. Vulkan-Verlag Essen, Ausgabe, Hrsg., 2004, Seite 160–172.
10. Sánchez, E., García-Ten, J., Ibáñez, M. J., Orts, M. J. and Cantavella, V., Polishing porcelain tile. Part 1. Wear mechanism. *Am. Soc. Ceram. Bull.* 2002, 50–54.
11. Wang, C. Y., Kuang, T. C., Qin, Z. and Wei, X., How abrasive machining affects surface characteristics of vitreous ceramic tile. *Am. Soc. Ceram. Bull.*, 2003, 9201–9208.
12. Fowles, G. R., *Analytical Mechanics*, 3rd edition. HOLT, RINEHART & WINSTON, 1986.